A new conceptual framework for assessing the physical state of the Baltic Sea

Urmas Raudsepp[1], Ilja Maljutenko[1], Priidik Lagemaa[1], Karina von Schuckmann[2]

[1] Department of Marine Systems, Tallinn University of Technology, Tallinn, 12618, Estonia
[2] Mercator Ocean international, 2 Av. de l'Aérodrome de Montaudran, 31400 Toulouse

Correspondence to: Ilja Maljutenko (ilja.maljutenko@taltech.ee)

Abstract.

A new conceptual framework for the assessment of the physical state of the general natural water basin was introduced and then tested for the Baltic Sea. The model includes the analysis of mutual variability of ocean heat content (OHC), freshwater content (FWC), subsurface temperature and salinity, atmospheric forcing functions along with salt transport across the open boundaries as well as river runoff. The random forest model was used as the main analyses tool to highlight statistical dependencies between state variables and potential forcing factors. Results show a distinct ocean warming trend in the Baltic Sea over a 30-year period, which covaried at interannual scale with air temperature at 2-meter height, evaporation and wind stress magnitude. Interannual changes of FWC were explained by large volume saline water inflows, net precipitation and zonal wind stress. This framework offers a new perspective of the potential impact of a shallowing mixed layer depth, resulting from sustained sensible heat flux changes at the air-sea interface, on salt export and the overall reduction of FWC in the Baltic Sea. The study brought up that interannual variations of temperature and salinity within the vertically extended halocline layer are major contributors to the OHC and FWC changes in the Baltic Sea.

Short Summary. In the last three decades, the Baltic Sea has experienced an increase in temperature and salinity. This trend aligns with the broader pattern of atmospheric warming. The significant warming and the yearly fluctuations in the ocean's heat content in the Baltic Sea are largely explained by subsurface temperature variations in the upper 100-meter layer, which includes the seasonal thermocline and the permanent halocline. These fluctuations are influenced by factors such as air temperature, evaporation, and the magnitude of wind stress. The changes in the sea's liquid freshwater content are primarily driven by salinity shifts within the halocline layer, which extends vertically from 40 to 120 meters depth. However, salinity changes in the upper layer play a minor role in the yearly variability of the freshwater content. The inflow of saline water, overall precipitation, and zonal wind stress are the principal factors affecting the freshwater content changes in the Baltic Sea.

1 Introduction

Amidst global warming, increased air temperatures have led to higher ocean water temperatures and the melt of land-based ice (IPCC, 2021). The former has caused a rise in Ocean Heat Content (OHC), while the latter has introduced significant amounts of freshwater into the ocean, contributing to the rise in global sea levels. In 2023, there was an exceptional increase in global sea surface temperature over the period 1973-2024 (McGrath et al., 2024), and OHC reached unprecedented levels (Cheng et al., 2024). In the Baltic Sea, the temperature trends for the period 1850-2008 show fast warming at the surface (~ 0.06 K decade^{-1}) and bottom (> 0.04 K decade^{-1}), and slow in the intermediate layers (< 0.04 K decade^{-1}) (Dutheil et al., 2023). Surface warming has progressively increased over time, primarily due to the sensible heat flux and latent heat flux (Kniebusch et al., 2019a). Trends in Fresh Water Content (FWC) are not as consistent globally as those of OHC (Boyer et al., 2007), although the rise in global sea level is widely acknowledged (Frederikse et al., 2020). Salinity patterns differ across various ocean regions of the world (Skliris et al., 2014), with the North Atlantic–North Pacific salinity contrast increasing by 5.9% ± 0.6% since 1965 (Lu et al., 2024). At a regional scale in the Baltic Sea, FWC has shown a significant downward trend over the last 30 years (Raudsepp et al., 2023). Windsor et al. (2001) demonstrated that long-term variations in the freshwater content (FWC) of the Baltic Sea are closely linked to accumulated changes in river runoff. Building on this work, Rodhe and Winsor (2002) concluded that the recycling of Baltic Sea water at the junction between the Baltic Sea and the North Sea is a crucial process in determining the sea's salinity. An increase in freshwater supply to the Baltic Sea will intensify water recycling, resulting in lower salinity, and vice versa.

The analysis of the physical state of natural water basins typically focuses on the evolution and spatial distribution of temperature and salinity and corresponding uncertainty estimations (Lindestroem et al. 2012), which are essential ocean variables (EOV). These variables are four dimensional and therefore provide spatially and temporarily resolved description of the state of the water body. Meanwhile, OHC and FWC are vital integral characteristics of the ocean, indicative of a water body's energy and mass, respectively. While OHC is a well-established indicator in ocean and climate research, its counterpart, ocean FWC, has received less attention.

We propose a new conceptual framework for assessing the physical state of the Baltic Sea by integrating multiple physical and statistical approaches (Fig. 1). The framework is based on two main physical indicators: OHC and FWC. These indicators are used to describe the energy and mass balance of the Baltic Sea. The study identifies the major variables affecting these indicators, including subsurface temperature, salinity, atmospheric forcing factors, and salt transport.

The framework follows a three-stage process: time-series analysis, depth-based variability analysis and causal relationships using machine learning. The initial phase consists of calculating the time series of OHC and FWC for the entire Baltic Sea. This provides insights into long-term trends and interannual variability. In basins covered partially by sea ice, the annual mean ice extent (MIE) is considered an important integral characteristic. The next step examines the horizontally averaged

vertical distribution of temperature (for OHC) and salinity (for FWC) to determine which depth ranges contribute the most to their variations. While this does not directly attribute causal links, the vertical profiles of temperature and salinity provide strong indications of which forcing factors might be responsible for changes in OHC and FWC. The final stage integrates forcing functions and ocean state characteristics to identify causal relationships. A Random Forest (RF) model is employed to highlight statistical dependencies between oceanic state variables and external forcing mechanisms. This machine-learning approach enables the identification of general patterns in the temporal evolution of the Baltic Sea's physical state.

Our proposed framework integrates the analysis of OHC and FWC by considering both their bulk integral values and their vertical distributions, allowing for the identification of key depth ranges contributing to their variability – which goes beyond other similar frameworks. Unlike the GOOS EOV framework (https://goosocean.org/), which focuses on structured global ocean monitoring without machine learning-based causal analysis, our approach explicitly incorporates machine learning to identify potential drivers of variability. Compared to the IPCC Climate and Ocean Monitoring Framework (IPCC AR6 (2021) Ocean Observations Chapter https://www.ipcc.ch/report/ar6/wg1/), which relies on dynamical climate models for global-scale processes, our framework is designed for regional-scale Baltic Sea analysis, offering a more localized and detailed assessment. Finally, while the NASA Salinity and Heat Budget Analysis (NASA Salinity Budget Project https://podaac.jpl.nasa.gov) is largely empirical and focused on global salinity and heat transport, our approach provides a structured three-stage methodology, incorporating not only empirical analysis but also a cause-and-effect exploration using machine learning. This makes our framework uniquely suited for regional climate monitoring and actionable insights into the physical state of the Baltic Sea.

This conceptual framework is designed as an indicator-based approach relevant to policymakers. It enables the monitoring of climate change impacts on the Baltic Sea while maintaining a balance between scientific rigor and practical accessibility. The framework is not meant to serve as a comprehensive dynamical model but rather as a scientifically robust tool for assessing the state of the Baltic Sea and guiding regional management decisions.

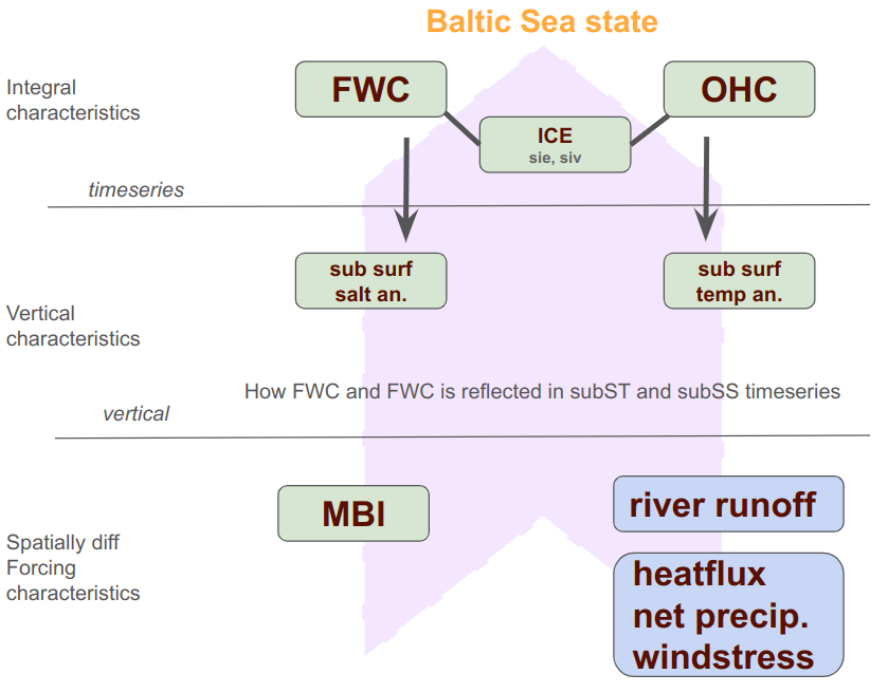

Figure 1: Conceptual Scheme of the Baltic Sea State parameters.

The study aims to evaluate a framework for assessing the physical state of the Baltic Sea by integrating annual mean values of OHC, FWC, subsurface temperature and salinity, atmospheric forcing functions, salt transport, and river runoff. The objective is to use a data-driven RF approach as the primary analysis tool to parse out nonlinear relationships and feature importances from a broad dataset. This study introduces an integrative, basin-wide approach, defining the entire Baltic Sea as a single water body for analysis. It computes a time series of total OHC and FWC for the whole sea. Rather than focusing solely on local variations, the methodology emphasizes these integrated indices as representations of the sea's overall state. This holistic integration marks a shift from the segmented or localized analyses of the past.

The Baltic Sea is recognized for its spatially pronounced heterogeneous structure. Its various subregions may exhibit distinct temporal variations in key state variables and overall dynamics, making it a complex environment for testing the conceptual framework. The Baltic Sea, a shallow marginal sea in northeastern Europe, is characterized by its hydrographic fields and sea ice conditions (Leppäranta and Myrberg, 2009). Salinity levels are affected by saline water inflows from the North Sea through the Danish straits, riverine freshwater inputs, and net precipitation (Lehmann et al., 2022). Major Baltic Inflows, which introduce saline and oxygen-rich water, are sporadic and unpredictable (Mohrholz, 2018). Temperature fields are influenced by the heat exchange with the atmosphere. The residence time of the Baltic Sea's water is several decades long (Meier et al., 2022). The vertical salinity stratification is defined by the halocline's depth, featuring a well-mixed surface layer and a slightly stratified layer beneath. Water temperature plays a crucial role in forming secondary stratification related

to the temperature of the upper mixed layer. Seasonal temperature cycles lead to partial freezing of the Baltic Sea in winter. Changes in sea ice extent over time are a vital indicator of climate change for the area. A reduction in maximum ice extent impacts the sea's vertical stratification and the seasonal trends in ocean heat and freshwater content (Raudsepp et al., 2022; 2023). Despite global warming, there has not been a significant increase in the Baltic Sea's relative sea level (Ranasinghe et al., 2021), which instead shows a strong seasonal cycle.

2 Data and methods

Table 1: Product Table

Product ref. no.	Product ID & type	Data access	Documentation
1	BALTICSEA_MULTIYEAR_PHY_003_011; Numerical models	EU Copernicus Marine Service Product (2023);	Quality Information Document (QUID): Panteleit et al. (2023); Product User Manual (PUM): Ringgaard et al. (2024)
2	ERA5; Numerical models	Copernicus Climate Change Service (2023)	Product reference: Hersbach et al., 2023 Journal article: Hersbach et al., 2020
3	E-HYPE; Numerical models	SMHI	Donnelly et al., 2016

2.1 Oceanographic and atmospheric data

The Baltic Sea physics reanalysis multi-year product (BAL-MYP; Table 1 product reference 1) is derived from the ocean model NEMO v4.0 (Gurvan et al., 2019). It assimilates satellite observations of sea surface temperature (SST) (EU Copernicus Marine Service Product, 2022) and in-situ temperature and salinity profiles from the ICES database (ICES Bottle and low-resolution CTD dataset, 2022). The model data is provided on a grid with a horizontal resolution of 1 nautical mile, including 56 vertical layers, covering the entire Baltic Sea and the transition zone to the North Sea. The dataset covers the period from 1993 to 2023, with the model setup detailed in the Product User Manual (PUM, Ringgaard et al., 2024).

The BAL-MYP has been extensively validated, as documented in the Quality Information Document (QuID; Panteleit et al., 2023), focusing on the period from 1st January 1993 to 31st December 2018. Additionally, the BAL-MYP data were evaluated using a clustering method with the K-means algorithm (Raudsepp and Maljutenko, 2022), which provided insights into the reanalysis accuracy by categorising errors (Lindenthal et al., 2023). Fifty-seven percent of the data are clustered with a bias of dS=-0.40 g/kg and dT=-0.02 °C, encompassing 57% of all data points with RMSE S=0.92 g/kg and T=0.54 °C. These points are distributed throughout the Baltic Sea. Clusters with high positive and negative temperature biases account

for 11% and 8% of total points, respectively, with marginal salinity biases and relatively even spatial distributions across the Baltic Sea. Twenty-six percent of the points have low temperature but high salinity errors, both negative and positive, predominantly located in the southwestern Baltic Sea, indicating occasional underestimation or overestimation of the inflow/outflow salinity.

OHC offers a comprehensive view of oceanic heat storage, crucial for evaluating climate change impacts, energy budgets, and long-term trends (Forster et al., 2024). OHC directly reflects Earth's energy imbalance, making it a key metric for tracking global warming, unlike basin-averaged temperature, which lacks a direct connection to energy budgets (von Schuckmann et al., 2016, 2023). Consequently, OHC is prioritized in climate models and international assessments (IPCC, 2019) due to its direct relationship with anthropogenic forcing and its predictive value for future climate scenarios. The daily OHC has been computed for each model grid cell from reanalysis (product reference 1), following the methodology of Meyssignac et al. (2019)

$$OHC = \rho * cp * (T + 273.15) \quad (1),$$

where ρ is the density of seawater calculated following the TEOS10 (IOC et al. 2010), cp is specific heat capacity calculated as a third order polynomial function of salinity and temperature according to Millero et al.(1973), T is daily temperature.

Ocean FWC is deemed more significant than mean salinity for understanding climate dynamics and ocean processes. FWC provides a holistic measure of freshwater storage and its effects on ocean circulation, climate, and sea-level rise (Solomon et al., 2021; Fukumori et al., 2021). It directly measures freshwater inputs (e.g., ice melt, river runoff, rainfall) or losses (e.g., evaporation), whereas mean salinity only indicates the average salt concentration, ignoring volume (Hoffman et al., 2023). A minor salinity change over a large water volume could signify a substantial freshwater flux, which mean salinity alone would not reveal (Schauer and Losch, 2019). The FWC was calculated at each grid point and day as Boyer et al. (2007)

$$FWC = \rho(Sref, Tref, p) / \rho(0, Tref, p) \cdot (Sref - S) / S \quad (2)$$

The three-dimensional temperature (Tref) and salinity (Sref) fields are temporal averages over the period of 1993–2023. A detailed description of the calculation procedure is available in Raudsepp et al. (2023). The OHC and FWC were calculated by spatially integrating the gridded OHC, (1), and FWC, (2), over the Baltic Sea, and then the annual mean OHC and FWC values were calculated from these daily values.

The Mixed Layer Depth (MLD), also referred to as the Upper Mixed Layer (UML), was included in the analysis using data from a multi-year reanalysis product (Table 1, Ref. 1). The MLD was calculated based on density stratification following the method of de Boyer Montégut et al. (2004), which defines MLD as the depth at which seawater density deviates from the reference density at 10 m depth by a specified threshold. For the Baltic Sea, this threshold was adjusted to 0.03 kg/m³ to better represent the characteristics of the regional upper mixed layer (Panteleit et al., 2023).

Atmospheric data were obtained from the ERA5 reanalysis (Table 1 product ref 2) for the period 1993–2023. The parameters included 2-meter air temperature, total precipitation, evaporation, wind stress magnitude, and the x- and y-components of wind stress, along with total cloud cover and surface net solar radiation. The time series for the annual mean values of these atmospheric parameters were computed as horizontal averages across the Baltic Sea region.

2.2 Random Forest

Random Forest (RF) is an ensemble learning method predominantly used for classification and regression tasks (Breiman, 2001). It functions by building multiple decision trees during the training phase and outputs the class that is the mode of the classes (classification) or the mean prediction (regression) of the individual trees. This method enhances accuracy and helps prevent overfitting, thus making it resilient to noise in the dataset. RF proves to be highly effective in analyzing complex interactions between variables, such as the relationships between marine state variables and atmospheric parameters. Its effectiveness is due to its capability to manage high-dimensional data and its resistance to outliers and noise, which are prevalent in environmental datasets. Additionally, RF is adept at detecting nonlinear relationships between predictor variables (atmospheric parameters) and response variables (marine state variables), which linear models often overlook.

In the context of an RF model, feature importance is a technique that identifies the most influential input features (variables) in predicting the output variable. The importance of each feature is determined by the decrease in model accuracy when the data for that feature is permuted, while all other features remain unchanged. If permuting a feature's values significantly increases the model's error, that feature is deemed crucial for the model's predictions. This approach aids in discerning the contribution of each feature to the model's decision-making process and in identifying key atmospheric parameters that significantly impact marine state variables. A positive value for a feature implies that permuting that predictor variable's values raises the model's prediction error, indicating the variable's importance for the model’s predictive accuracy. A higher positive value suggests greater reliance on that variable by the model.

In this study we have trained the four different RF models to fit the OHC and FWC timeseries with the hyperparameter configurations shown in Table 2. Two models are trained to predict the OHC and FWC values from the set of the meteorological variables (*var* suffix) and two from the horizontally averaged temperature and salinity profiles (*zax* suffix). To optimize the performance of the RF models while ensuring robustness and generalizability, a set of hyperparameters was selected based on sensitivity analysis conducted for number and depth of the trees (Fig A2). The minimum leaf size (MinLS) was set to 1, allowing the trees to fully grow and capture complex data patterns. The number of predictors to sample at each split (Pred2Samp) was dynamically determined as one-third of the total number of predictors, tackling a balance between feature randomness and predictive strength. This approach promotes diversity among trees while preventing excessive correlation. The number of trees (NumTrees) in each RF model was set to 100, providing sufficient ensemble stability while maintaining computational efficiency. Since this study employs RF models to investigate nonlinear relationships between predictors and state variables, we use the entire dataset as the training set to maximize the models' ability to learn patterns.

To further enhance predictive reliability, assess uncertainty, and evaluate the stability of both predictions and feature importances, an ensemble of 150 independently trained RF models was constructed.

We employed MATLAB's TreeBagger function to assess the feature importance of atmospheric predictors on marine state variables. The `OOBPermutedPredictorDeltaError` method, a robust metric from MATLAB's TreeBagger, quantifies each predictor's importance via the out-of-bag (OOB) prediction error. This involves permuting each variable's values across OOB observations for each tree. The resulting change in prediction error from these permutations is calculated for each tree. These measures are averaged across all trees and normalised by the standard deviation of the changes, providing a standardised score that highlights the variables with the most significant impact on predictive accuracy. Averaging the feature importance scores across all 150 models minimises the noise and variability from any single model's training, offering a more consistent and dependable indication of each atmospheric parameter's contribution to predicting marine state variables.

Table 2. Hyperparameter configurations for different Random forest models

Model	NumTrees	MinLS	Pred2Samp	Ens
RF_OHC*zax*	100	1	14	150
RF_OHC*var*	100	1	3	150
RF_FWC*zax*	100	1	14	150
RF_FWC*var*	100	1	4	150

3 Results

Both OHC and FWC display a statistically significant linear trend, as shown in Figure 2. Using a z-score time series allows for the comparison of trends per year (trend*) and data distributions without the influence of their units. OHC shows an increasing trend* of 0.089±0.025, while FWC exhibits a decreasing trend* of -0.092±0.023, both comparable in magnitude (Table 3). The corresponding absolute values are 0.34±0.095 W/m^2 for OHC and -36.99±9.20 km^3/year for FWC (Table 3). Between 1993 and 2003, OHC and FWC varied similarly, both rising and falling concurrently (blue dots in Fig. 2). After this period, their patterns diverged (yellow and red dots in Fig.2). Interannual variations of the annual mean sea ice extent and OHC are strongly correlated but in opposite phases. Among the forcing functions, the 2-meter air temperature shows a distinct positive trend (Fig. 2), albeit weaker than the trends of OHC and FWC (Table 3). The air temperature over the Baltic Sea area has risen with trend* of 0.074±0.031 (Table 3). Surface net solar radiation has a weaker but still significant positive trend* of 0.058±0.035, and the evaporation time series shows a negative trend* of -0.041±0.039 (Fig. 2, Table 3). Other

atmospheric variables did not exhibit statistically significant trends (Fig. 2). Correlation coefficients among various atmospheric datasets were generally low (Table 4). The two highest correlation coefficients, 0.76 and 0.73, are between wind stress magnitude and its zonal component, indicating a predominance of westerly airflow over the Baltic Sea, and between 2-meter air temperature and surface net solar radiation, respectively. The low correlations suggest a weak statistical relationship between the annual mean atmospheric parameters, supporting the inclusion of all forcing functions in the RF model.

Table 3. Linear annual trend values of z-scored time series (trend*), standard deviation (STD), linear trend of physical value (Unit/year, except for OHC) and mean value (mean) of original time series. *OHC*: ocean heat content, *FWC*: fresh water content, *T2*: 2 metre temperature, *TP*: total precipitation, *EVAP*: evaporation, *Wstr*: windstress, *WUstr*: windstress u component, *WVstr*: windstress v component, *TCC*: total cloud cover , *SSR*: surface net solar radiation, *RNF*: river runoff.

Variable:	OHC	FWC	T2	TP	EVAP	Wstr	WUstr	WVstr	TCC	SSR	RNF
Unit	MJ/m²	km³	°C	m/y	m/y	N/m²	N/m²	N/m²	1	W/m²	m³/s
trend*:	0.089 ± 0.025	-0.092 ± 0.023	0.074 ± 0.031	0.032 ± 0.04	-0.041 ± 0.039	-0.0016 ± 0.0418	0.013 ± 0.041	0.015 ± 0.041	-0.0077 ± 0.0417	0.058 ± 0.035	0.0073 ± 0.0417
STD:	122.02	402.00	0.73	0.071	0.041	0.0056	0.0100	0.0072	0.0226	3.16	1,687.92
trend:	0.344 (W/m²)	-36.987	0.054	0.0023	-0.0016	-8.85×10^{-6}	1.32×10^{-4}	1.05×10^{-4}	-1.75×10^{-4}	0.18	12.31
mean:	60.20	-63.73	7.65	0.73	-0.55	0.0999	0.0244	0.0138	0.6493	113.92	17,807.77

Table 4. Correlations coefficients (lower triangle) and StandardErrors (Gnambs, 2023) (upper triangle) of atmospheric parameters. Correlation coefficients which pass two-tailed t-test at 95% confidence are in bold. *OHC*: ocean heat content, *FWC*: fresh water content, *T2*: 2 metre temperature, *TP*: total precipitation, *EVAP*: evaporation, *Wstr*: wind stress magnitude, *WUstr*: wind stress u component, *WVstr*: wind stress v component, *TCC*: total cloud cover , *SSR*: surface net solar radiation.

	T2	*TP*	*EVAP*	*Wstr*	*WUstr*	*WVstr*	*TCC*	*SSR*
T2		0.19	0.17	0.17	0.15	0.14	0.15	0.09
TP	0.12		0.18	0.17	0.18	0.18	0.13	0.17
EVAP	-0.28	-0.18		0.19	0.18	0.16	0.19	0.15
Wstr	0.31	0.35	-0.10		0.08	0.15	0.18	0.19
WUstr	**0.47**	0.25	0.16	**0.76**		0.15	0.16	0.18
WVstr	**0.48**	0.16	0.37	**0.43**	**0.43**		0.19	0.19
TCC	-0.43	**0.58**	-0.04	-0.20	-0.42	-0.13		0.09
SSR	**0.73**	-0.31	-0.43	0.07	0.18	0.11	-0.73	

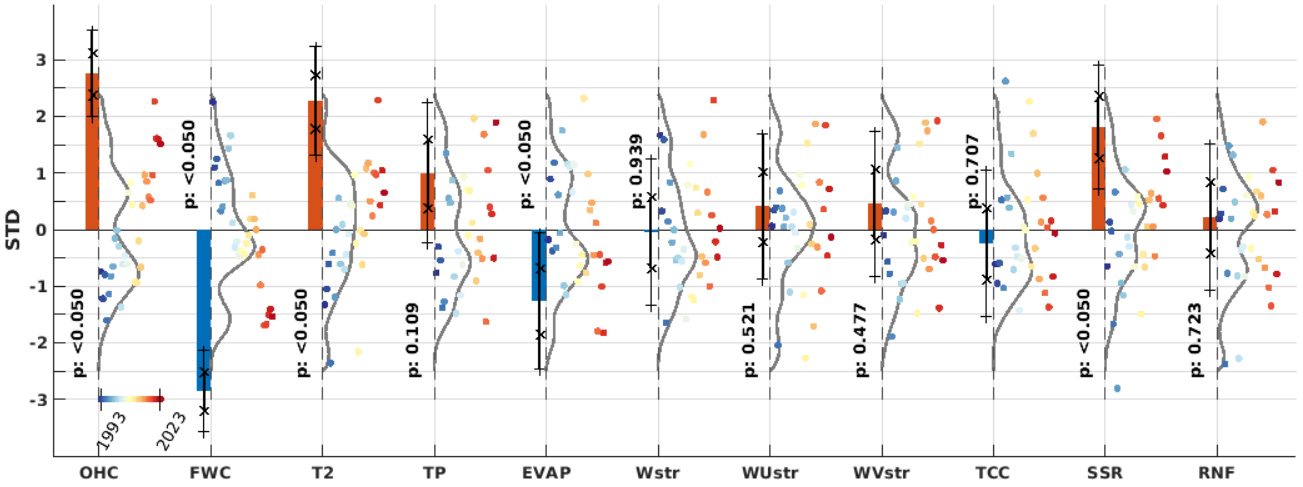

Figure 2: Trend analysis and probability distribution functions (PDFs) of the annual time series of standardized (*z-scores) Baltic Sea state and meteorological parameters. To the left of the dashed line, the period-normalized annual trend values (multiplied by the period length in years i.e. 30) are displayed as red (positive) and blue (negative) bars with corresponding p-values (95% confidence level), along with whiskers representing ±1 standard error (x ticks) and the 95% uncertainty range (+ ticks). On the right side from the dashed line, probability density functions (PDFs) are shown as the solid lines for the standardized time series, which are represented by colored dots. The color of the dots represents the year on a common color scale shown at the OHC variable.
For each dashed axis following variable stands *OHC*: ocean heat content, *FWC*: fresh water content, *T2*: 2 metre temperature, *TP*: total precipitation, *EVAP*: evaporation, *Wstr*: windstress, *WU/WVstr*,: windstress u and v component, *TCC*: total cloud cover , *SSR*: surface net solar radiation, *RNF*: river runoff.

In analyzing OHC variations, we use a RF model. This model employs horizontally averaged annual temperature values at each depth level, derived from the depth levels of a multi-year product (Table 1 product ref 1), as input features. The RF model finely replicates the annual OHC time series (Fig 3a), with high correlation coefficient (0.986) and a RMSD of the standardized time series at 0.0016. However, it did not capture the extreme OHC event in 2020 or the low OHC extreme in 1996 (Fig. 3). Feature importance is significant within a depth range of 10-80 meters (Fig. 3b), with two peaks at depths of 18 and 60 meters, aligning with the average depths of the seasonal thermocline and the permanent halocline, respectively. This suggests that interannual OHC variations are mainly influenced by temperature changes within these layers. Subsurface temperatures from 1993 to 2023 indicate warming trends of approximately 0.06 °C/year across all depths (CMS 2024a). From 1993 to 1997, deep water temperatures remained relatively low (below 6 °C). Since 1998, deeper waters have warmed, with temperatures above 7 °C occupying the layer below 100 meters since 2019. The water temperature below the halocline has risen by about 2 °C since 1993, and the cold intermediate layer's temperature has also increased during the 1993-2023 period.

A similar method is employed to elucidate the inter-annual fluctuations of FWC, utilizing horizontally averaged salinity at each depth level. The model's precision is slightly lower (Correlation: 0.973, RMSD of standardized time series: 0.004) compared to that for OHC. The model consistently underperforms in predicting the FWC peaks, encompassing both the lows and highs (Fig. 3c). The most notable features cover the depth range of 40-120 meters (Fig. 3d), coinciding with a halocline layer and its vertical extensions to both shallower and deeper depth. The salinity levels at the bottom layer are of secondary importance to the inter-annual variations of FWC in the Baltic Sea. The salinity in the top 25-meter stratum exerts a minimal influence on FWC changes. The interannual variability of salinity in the upper stratum is minor relative to the deeper stratum. The salinity gradient ascends steadily from zero at a depth of 25 meters to 0.04 g/kg annually at 70 meters (CMS 2024b). The most marked trend, 0.045 g/kg per annum, occurs within the expanded halocline layer extending from 70 to 150 meters. Notably, there is a slight dip in the salinity trend to 0.04 g/kg per annum between the depths of 150 and 220 meters. While this reduction is slight, it indicates that salt influx into the expanded halocline layer is more significant than into the deeper strata. A salinity trend of 0.05 g/kg annually is detected in the deepest stratum of the Baltic Sea.

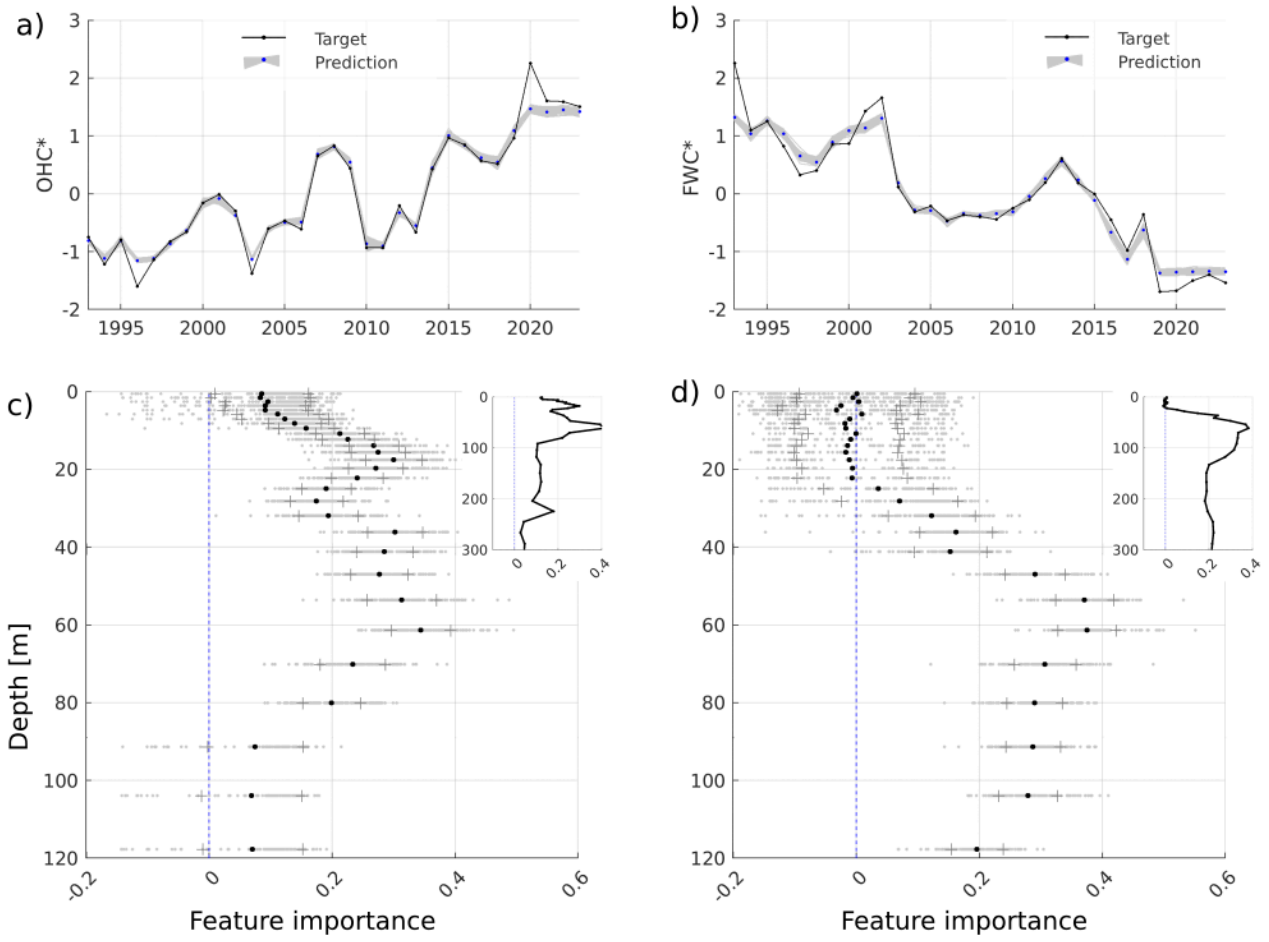

Figure 3: OHC* and FWC* ensemble predictions (ens. mean as blue dots) using the horizontal average salinity and temperature profiles (a), (b). The prediction features importance, with ensemble spread (1 STD shown with "+" marker), for each depth in the upper 120 m layer shown on c) and d) and for full depth range in the upper-right inset panels. All variables are z-scored.

Building a RF model targeting OHC and FWC timeseries with atmospheric forcing functions reveals the 2-meter air temperature as the most significant contributor (Appendix 1). This correlation is physically plausible for OHC but less so for FWC. The 2-meter air temperature affects the air-sea heat exchange via the sensible heat flux component. To further explore the declining FWC trend, we examined interannual changes in the annual average upper mixed layer depth (MLD). In the Baltic Sea, MLD varies widely across different areas and seasons. A shallowing of MLD is observed in the Baltic Proper and to some extent in the Bothnian Sea, while a MLD deepening is noted in the Bothnian Bay, the Gulf of Finland, and the Gulf of Riga. Typically, the Baltic Sea's stratification is influenced by salinity, although a seasonal thermocline forms across the sea. In the northern and eastern basins, the dispersal of river water during spring and summer leads to the development of the

seasonal pycnocline. Conversely, in the southern Baltic Sea, the spread of river water is mostly restricted to the coastal areas, so the mixed layer is less affected by the seasonal halocline.

We performed test experiments with the RF model, incorporating the upper mixed layer (UML) as an additional feature. We determined the annual mean UML depth across the Baltic Sea and specifically for the Eastern Gotland Basin. The decline in the UML depth was more significant in the Eastern Gotland Basin compared to the entire Baltic Sea. The UML depth in the Eastern Gotland Basin decreased from 30 meters in 1993 to 22 meters in 2023. The MLD feature became more significant than the 2-meter temperature in explaining the FWC when we considered the UML depth in the Eastern Gotland Basin. However, the results were contentious when we applied the average UML depth for the entire Baltic Sea. An increase in the 2-meter temperature may cause a shallower mixed layer, potentially reducing the mixing between the surface freshwater layer and the denser saline layer beneath.

By eliminating trends, we utilized RF models to identify the primary characteristics of the interannual fluctuations of OHC and FWC. The ensemble mean forecast of OHC effectively captures these interannual changes (Fig. 4a), evidenced by a correlation coefficient of 0.9012 and a RMSD of 0.3432. Factors such as 2-meter temperature, wind stress, and evaporation significantly influence the interannual variability of OHC (Fig. 4c). Additionally, total cloud cover and solar radiation have a minor impact on the shape of OHC.

In the FWC model, we incorporated bottom salinity from the Bornholm Basin as a supplementary feature. The direct calculation of salt transport from model data across a section at the Baltic Sea entrance is error-prone. Utilizing daily average cross-section velocities and salinities overlooks high-frequency fluctuations with considerable residual salt flux. The model's precision in predicting accurate salinity levels at the Baltic Sea's entrance is quite low (Lindenthal et al., 2024). Time series of bottom salinity changes in the Arkona and Bornholm Basins facilitate the tracking of the intermittent nature of water inflow and outflow events. The Arkona Basin, being relatively shallow, is known for its dynamic nature regarding volume and salt transport. Here, bottom salinity reflects the salinity shifts caused by inflow and outflow variations at the Baltic Sea entrance. These variations mask the large volume inflows chiefly responsible for the Baltic Sea's salt influx, thus not significantly affecting the Arkona Basin's bottom salinity over time. Conversely, the Bornholm Basin's greater depth means its bottom salinity is less affected by the upper layer's varying salinity water movements. Hence, the Bornholm Basin's bottom salinity serves as a more accurate indicator of the Baltic Sea's salt inflow. We also factored in the annual average river runoff (Table 1 product ref 3) into the Baltic Sea in our RF model.

The ensemble mean predictions of the FWC are marginally less precise, with a correlation coefficient of 0.8994 and a root mean square difference of 0.3624. Notable peaks in the FWC occurred in 1993, 2002, and 2013, each followed by a swift decline in subsequent years (Fig. 4b). The bottom salinity in the Bornholm Basin, serving as an indicator for salt flux into the Baltic Sea, along with total precipitation and the zonal wind component, are the primary factors influencing the FWC's interannual variations (Fig. 4d). Riverine freshwater discharge does not impact the FWC's interannual variations. A reduction

in FWC is associated with an increase in water salinity. The rise in the Baltic Sea's salinity is attributed to the transport of saline water through the Danish straits. The highest values of bottom salinity align with the Major Baltic Inflows of 1993, 2002, and 2014.

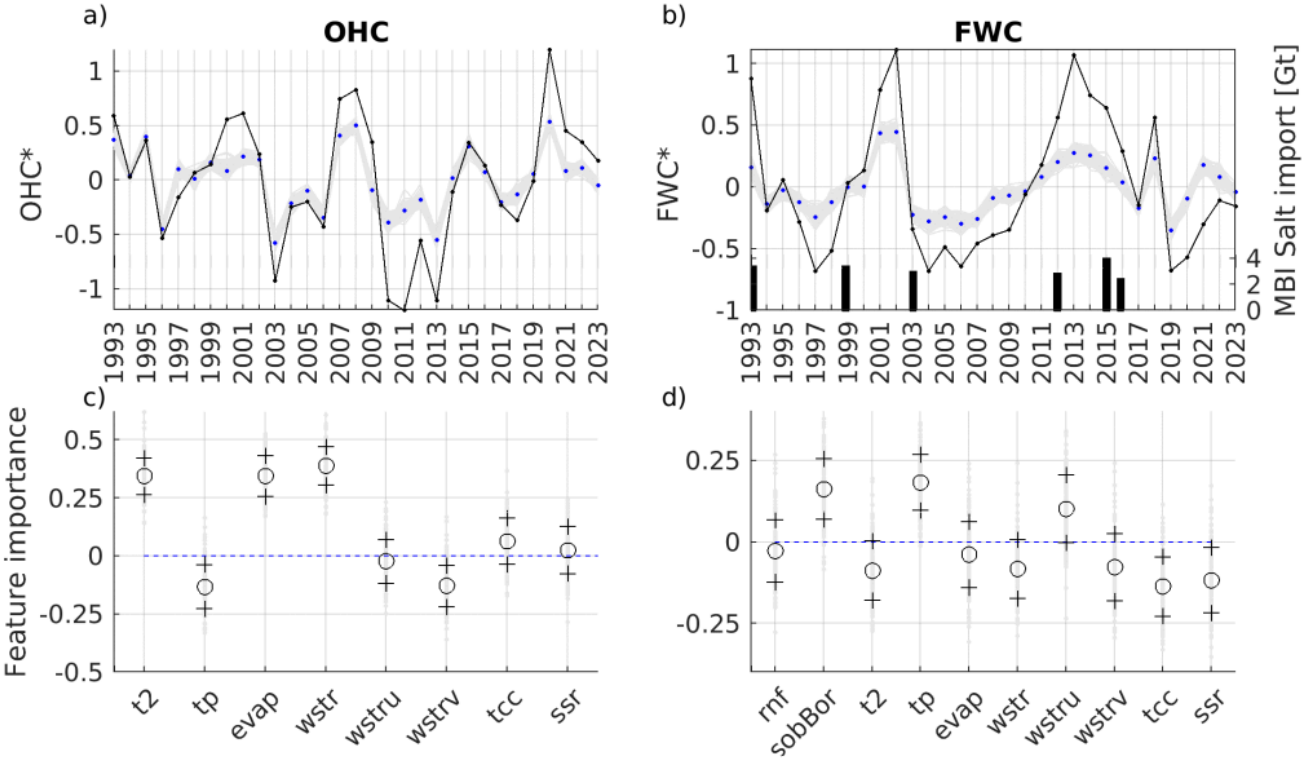

Figure 4: Time series of detrended OHC* (a) and FWC* (b) ensemble predictions (ens. mean as blue dots) using RF ensembles. Ensembles of corresponding models feature importances with ensemble spread ("+" markers corresponding to 1 STD) shown on (c) and (d) for OHC and FC respectively. All variables are z-scored. *OHC*: ocean heat content, *FWC*: fresh water content, *T2*: 2 metre temperature, *TP*: total precipitation, *EVAP*: evaporation, *Wstr*: windstress, *WU/WVstr*: windstress u and v component, *TCC*: total cloud cover, *SSR*: surface net solar radiation, *RNF*: river runoff, *sobBor*: bottom salinity in the deepest location of the Bornholm basin.

4. Discussion and Conclusions

We proposed a new conceptual framework in which the Baltic Sea's state is defined by two main factors: OHC and FWC. OHC and FWC are proposed as key descriptors of the Baltic Sea's physical state because they encapsulate the overall thermal and haline content of the entire basin. While temperature and salinity at specific locations or layers provide detailed information, OHC and FWC offer a high-level integration of those details. This integration is particularly useful for monitoring long-term trends and basin-wide changes, which is why we argue that OHC and FWC effectively define the large-scale physical state.

We employed the RF model (Breiman, 2001) to link the atmospheric and hydrologic variables with the variability of OHC and FWC. Our analysis across the entire Baltic Sea reveals the direct impact of atmospheric forcing on ocean warming. Moreover, this framework provides new insights into the role of salt import/export in FWC's interannual variability, and draws on the basin-wide decline of FWC, elevating the potential role of a flatting MLD from long-term sensible flux change at the air-sea interface. Particularly, results reveal that the Baltic Sea has undergone substantial change over the past decade as evidenced by the increase in OHC over the last thirty years.

Simultaneously, there has been a reduction in FWC, suggesting an increase in seawater salinity. The analysis of average subsurface temperature and salinity indicates that interannual variations in OHC and FWC are mainly influenced by temperature shifts in both the seasonal thermocline and permanent halocline and changes in salinity within the permanent halocline. This highlights the critical need for a comprehensive framework while reporting on the state of the Baltic Sea, allowing for the evaluation of basin-wide conditions, including its trends, interannual variations, and extremes, as well as the factors driving these changes. Using this approach could prove to be a valuable asset for the science-policy interface, aiding in regional evaluations of the sea state. .

Previous studies have reported a positive trend in OHC and a negative trend in FWC (Raudsepp et al., 2022; 2023), along with an inverse relationship between OHC and the maximum ice extent in the Baltic Sea (Raudsepp et al., 2022). The increase in OHC has been attributed to the rising air temperature over the Baltic Sea, yet the decline in FWC remains largely unexplained. Raudsepp et al. (2023) noted that neither salt transport to the Baltic Sea, net precipitation, nor total river runoff accounted for the FWC's downward trend. Despite this, deepwater salinity in the central Baltic Sea has been increasing at a rate of 0.2–0.25 g kg^{-1} per decade (Lehmann et al., 2022). A basin-wide analysis linking FWC changes to atmospheric forces revealed a relation with air temperature, a connection that is physically tenuous, prompting further investigation into other factors. This led to the hypothesis that the decreasing trend in the upper mixed layer thickness in the Baltic Sea might be influencing FWC changes. Over the last three decades, there has been a noticeable reduction in the upper mixed layer depth. While it is plausible to suggest a dynamic relationship between the shrinking mixed layer depth and the decrease in FWC, verifying this hypothesis requires more research than what is covered in the present study.

Interannual variations of OHC are influenced by air temperature, evaporation, and wind stress magnitude over the Baltic Sea (Fig. 4). When considering the lesser impact of total cloud cover and surface net solar radiation, it becomes clear that air-sea heat exchange primarily drives OHC changes in the Baltic Sea. Notably, the annual mean OHC parallels the long-term trend of winter OHC in the Baltic Sea's upper 50-m layer (Raudsepp et al., 2022), highlighting the influence of seasonal ice cover on OHC fluctuations. In seas with seasonal ice cover, the characteristics of sea ice are crucial for determining the sea's physical state. Typically, the maximum sea ice extent in the Baltic Sea indicates the severity of the winters (Uotila et al., 2015). Sea ice is vital for temporarily storing ocean heat and freshwater, then releasing it back into the sea.

The interannual variations of FWC were associated with Major Baltic Inflows, overall precipitation, and zonal wind stress (Fig. 4 d)). The signals of the MBIs are evident in the bottom salinity of the Bornholm Basin. Fig. 4 d) illustrates that interannual variations in FWC are linked to the bottom salinity in the Bornholm Basin, which serves as a proxy for MBIs, as well as zonal wind stress and net precipitation. Therefore, Fig. 4 d) highlights the drivers of FWC, while Fig. 3 d) emphasizes the significance of halocline salinity's response to FWC. Consequently, we can infer that inflows from the North Sea and net precipitation are responsible for changes in halocline salinity, with zonal wind facilitating these inflows. However, we were unable to directly associate moderate and small inflows from the North Sea with changes in halocline salinity. This aspect requires further investigation and precise simulation of salt transport between the North Sea and the Baltic Sea, which is beyond the scope of the current study.

Major Baltic Inflows inflows are crucial in shaping the hydrophysical conditions of the central Baltic Sea's deep regions, significantly affecting marine ecology across various trophic levels (Bergen et al., 2018). Without Major Baltic Inflows, the deeper layers of the central Baltic become oxygen-depleted, leading to the emergence of hydrogen sulphide (as noted by Savchuk, 2018). Furthermore, increased water temperatures have hastened oxygen depletion, causing the hypoxic areas to expand (Safonova et al., 2024). Consequently, the ongoing reduction in FWC and the rise in OHC signal a growth in the hypoxic and anoxic zones within the Baltic Sea.

Meier and Kauker (2003) demonstrated that increasing westerly winds could hinder the outflow of freshwater from the Baltic Sea, leading to decreased salt transport into the sea. While several studies have underscored a correlation with river runoff (Kniebusch et al., 2019b; Radtke et al., 2020; Lehmann et al., 2022), our research did not find this connection.

The OHC exhibits oscillations with a period of 5-7 years, reaching a high extreme in 2020 and a low extreme in 2011 (Fig. 4). The period from January to March 2020 was notably warm over the Northern Hemisphere (Schubert et al., 2022), which was evident in the Baltic Sea's winter OHC (Raudsepp et al., 2022). Additionally, the year 2020 was marked by an exceptionally high marine heatwave index (Bashiri et al., 2024) and a significant number of marine heatwave days (Lindenthal et al., 2024). Conversely, 2011 saw the greatest sea ice extent and volume of the past three decades (Raudsepp et al., 2022). Notably, high extremes in FWC, such as those in 2002 and 2013 (Fig. 4 b)), precede Major Baltic Inflow events, whereas low extremes, such as those in 1997 and 2019, follow several years after these events.

Global warming, with its increased frequency and intensity of extreme events, has had widespread negative impacts on nature and significant socioeconomic repercussions (IPCC, 2021). Our methodology has highlighted the extremes of interannual variability in OHC and FWC. In our study, we utilized the RF model to investigate the relationships between changes in OHC and FWC and their potential drivers. Although the model pinpointed the primary factors, it failed to capture the extremes (Gnecco et al., 2024), as illustrated in Fig. 4a,b. RF models tend to underperform when extreme values are not well-represented in the training data, a common issue in ecological modeling and other practical applications (Fox et al., 2017). This can result in a bias where the model does not recognize or accurately predict rare but impactful events, such as

extreme weather conditions, uncommon species occurrences, or anomalies in financial markets (Fox et al., 2017). Acknowledging this, we hypothesize that while primary forces set the stage for extreme events, these events themselves fall outside the scope of standard interannual variability and stem from a distinct combination of forces. Consequently, it is advantageous to analyze extreme events independently from typical interannual variations (Nontapa et al., 2020; Chen et al., 2021). To account for the variations in OHC and FWC, models other than RF, such as deep machine learning models, could be employed, especially if the temporal resolution is monthly (e.g., Barzandeh et al., 2024) or finer, ensuring a representative dataset is available. Advancing this methodology will further our comprehension of the causes behind extreme events, thereby improving our predictive abilities.

Data Availability

This study is based on public databases and the references are listed in Table 1.

Author contribution

UR designed the conceptual framework for this study, interpreted the results, and wrote the initial manuscript. **IM** performed the calculations of OHC and FWC, trained the RF models, and prepared the figures; **IM** also contributed to the manuscript development. **PL** and **KvS** contributed to the design of the framework and the presentation of the results. All authors contributed to writing and revising the manuscript.

Competing Interests

The authors declare that they have no conflict of interest.

Disclaimer

The Copernicus Marine Service offering is regularly updated to ensure it remains at the forefront of user requirements. In this process, some products may undergo replacement or renaming, leading to the removal of certain product IDs from our catalogue.

If you have any questions or require assistance regarding these modifications, please feel free to reach out to our user support team for further guidance. They will be able to provide you with the necessary information to address your concerns and find suitable alternatives, maintaining our commitment to delivering top-quality services.

References

Barzandeh, A., Maljutenko, I., Rikka, S., Lagemaa, Männik, A., P., Uiboupin, R., Raudsepp, U.: Sea surface circulation in the Baltic Sea: decomposed components and pattern recognition. Sci. Rep., 14, 18649, https://doi.org/10.1038/s41598-024-69463-8, 2024

Bashiri, B., Barzandeh, A., Männik, A., Raudsepp, U.: Marine heatwaves' characteristics and assessment of their potential drivers in the Baltic Sea over the last 42 years. Sci. Rep. (submitted), 2024

Bergen, B., Naumann, M., Herlemann, D.P.R., Gräwe, U., Labrenz, M., Jürgens, K.: Impact of a major inflow event on the composition and distribution of bacterioplankton communities in the Baltic Sea. Front. Mar. Sci., 5, 383, https://doi.org/10.3389/fmars.2018.00383, 2018

de Boyer Montégut, C., Madec, G., Sok Fischer, A., Lazar, A, Iudicone, D.: Mixed layer depth over the global ocean: An examination of profile data and a profile-based climatology, J. Geophys. Res., 109, C12003, doi: 0.1029/2004JC002378, 2004

Boyer, T., Levitus, S., Antonov, J., Locarnini, R., Mishonov, A., Garcia, H., Josey, S.A.: Changes in freshwater content in the North Atlantic Ocean 1955–2006. Geophys. Res. Lett., 34, L16603, https://doi.org/10.1029/2007GL030126, 2007

Breiman, L.: Random forests. Mach. Learn., 45, 5–32, https://doi.org/10.1023/A:1010933404324, 2001

Chen, S., Ren, M., Sun, W.: Combining two-stage decomposition based machine learning methods for annual runoff forecasting. J. Hydrol., 603B, 126945, https://doi.org/10.1016/j.jhydrol.2021.126945, 2021

Cheng, L., von Schuckmann, K., Minière, A., Schmidt, G.A., Pan, Y.: Ocean heat content in 2023. Nat. Rev. Earth Environ., 5, 232–234, https://doi.org/10.1038/s43017-024-00539-9, 2024

Copernicus Climate Change Service: ERA5 hourly data on single levels from 1940 to present. Copernicus Climate Change Service (C3S) Climate Data Store (CDS), https://doi.org/10.24381/cds.adbb2d47, last access: 4 April 2024

CMS: Baltic Sea subsurface temperature trend from reanalysis. E.U. Copernicus Marine Service Information (CMEMS) Marine Data Store (MDS), https://doi.org/10.48670/moi-00208, 2024a

CMS: Baltic Sea subsurface salinity trend from reanalysis. E.U. Copernicus Marine Service Information (CMEMS) Marine Data Store (MDS), https://doi.org/10.48670/moi-00207, 2024b

Donnelly, C., Andersson, J.C., Arheimer, B.: Using flow signatures and catchment similarities to evaluate the E-HYPE multi-basin model across Europe. Hydrol. Sci. J., 61, 255–273, https://doi.org/10.1080/02626667.2015.1027710, 2016

Dutheil, C., Meier, H.E.M., Gröger, M. et al.: Warming of Baltic Sea water masses since 1850. Clim Dyn 61, 1311–1331. https://doi.org/10.1007/s00382-022-06628-z, 2023

EU Copernicus Marine Service Product: Baltic Sea - L3S Sea Surface Temperature Reprocessed. Mercator Ocean Int., https://doi.org/10.48670/moi-00312, 2022

EU Copernicus Marine Service Product: Baltic Sea physics reanalysis. Mercator Ocean Int., https://doi.org/10.48670/moi-00013, 2023.

Frederikse, T., Landerer, F., Caron, L., Adhikari, S., Parkes, D., Humphrey, V.W., Dangendorf, S., Wu, Y.-H.: The causes of sea-level rise since 1900. Nature, 584, 393–397, https://doi.org/10.1038/s41586-020-2591-3, 2020.

Forster, P. M., Smith, C., Walsh, T., Lamb, W. F., Lamboll, R., Hall, B., Hauser, M., Ribes, A., Rosen, D., Gillett, N. P., Palmer, M. D., Rogelj, J., von Schuckmann, K., Trewin, B., Allen, M., Andrew, R., Betts, R. A., Borger, A., Boyer, T., Broersma, J. A., Buontempo, C., Burgess, S., Cagnazzo, C., Cheng, L., Friedlingstein, P., Gettelman, A., Gütschow, J., Ishii, M., Jenkins, S., Lan, X., Morice, C., Mühle, J., Kadow, C., Kennedy, J., Killick, R. E., Krummel, P. B., Minx, J. C., Myhre, G., Naik, V., Peters, G. P., Pirani, A., Pongratz, J., Schleussner, C.-F., Seneviratne, S. I., Szopa, S., Thorne, P., Kovilakam, M. V. M., Majamäki, E., Jalkanen, J.-P., van Marle, M., Hoesly, R. M., Rohde, R., Schumacher, D., van der Werf, G., Vose, R.,

Zickfeld, K., Zhang, X., Masson-Delmotte, V., and Zhai, P.: Indicators of Global Climate Change 2023: annual update of key indicators of the state of the climate system and human influence, Earth Syst. Sci. Data, 16, 2625–2658, https://doi.org/10.5194/essd-16-2625-2024, 2024.

Fox, E.W., Hill, R.A., Leibowitz, S.G., Olsen, A.R., Thornbrugh, D.J., Weber, M.H.: Assessing the accuracy and stability of variable selection methods for random forest modeling in ecology. Environ. Monit. Assess., 189, 316, https://doi.org/10.1007/s10661-017-6025-0, 2017

Fukumori, I., Wang, O., Fenty, I, Causal Mechanisms of Sea Level and Freshwater Content Change in the Beaufort Sea. Journal of Physical Oceanography, 51, 3217-3234, DOI: 10.1175/JPO-D-21-0069.1, 2021

Gnambs, T.: A brief note on the standard error of the Pearson correlation. Collabra Psychol., 9, 1–7, https://doi.org/10.1525/collabra.87615, 2023

Gnecco, N., Terefe, E.M., Engelke, S.: Extremal random forests. J. Am. Stat. Assoc., 1–14, https://doi.org/10.1080/01621459.2023.2300522, 2024

EOV: Essential ocean variables. EOV, https://goosocean.org/what-we-do/framework/essential-ocean-variables/, accessed on 4 September 2024

Gurvan, M., Bourdallé-Badie, R., Chanut, J., et al.: NEMO ocean engine. Notes du Pôle de modélisation de l'Institut Pierre-Simon Laplace (IPSL), v4.0, Number 27, https://doi.org/10.5281/zenodo.3878122, 2019

Hersbach, H., Bell, B., Berrisford, P., Hirahara, S., Horányi, A., Muñoz-Sabater, J., Nicolas, J., Peubey, C., Radu, R., Schepers, D., Simmons, A., Soci, C., Abdalla, S., Abellan, X., Balsamo, G., Bechtold, P., Biavati, G., Bidlot, J., Bonavita, M., De Chiara, G., Dahlgren, P., Dee, D., Diamantakis, M., Dragani, R., Flemming, J., Forbes, R., Fuentes, M., Geer, A., Haimberger, L., Healy, S., Hogan, R.J., Hólm, E., Janisková, M., Keeley, S., Laloyaux, P., Lopez, P., Lupu, C., Radnoti, G., de Rosnay, P., Rozum, I., Vamborg, F., Villaume, S., Thépaut, J.-N.: Complete ERA5 from 1950: Fifth generation of ECMWF atmospheric reanalyses of the global climate. Copernicus Climate Change Service (C3S) Data Store (CDS), 2023

Hersbach, H., Bell, B., Berrisford, P., Hirahara, S., Horányi, A., Muñoz-Sabater, J., Nicolas, J., Peubey, C., Radu, R., Schepers, D., Simmons, A., Soci, C., Abdalla, S., Abellan, X., Balsamo, G., Bechtold, P., Biavati, G., Bidlot, J., Bonavita, M., De Chiara, G., Dahlgren, P., Dee, D., Diamantakis, M., Dragani, R., Flemming, J., Forbes, R., Fuentes, M., Geer, A., Haimberger, L., Healy, S., Hogan, R.J., Hólm, E., Janisková, M., Keeley, S., Laloyaux, P., Lopez, P., Lupu, C., Radnoti, G., de Rosnay, P., Rozum, I., Vamborg, F., Villaume S., Thépaut, J.-N.: The ERA5 global reanalysis. Q. J. R. Meteorol. Soc., 146, 1999–2049, https://doi.org/10.1002/qj.3803, 2020

Hoffman, E. L., Subrahmanyam, B., Trott, C. B., Hall, S. B. Comparison of Freshwater Content and Variability in the Arctic Ocean Using Observations and Model Simulations. Remote Sensing, 15(15), 3715. https://doi.org/10.3390/rs15153715, 2023

ICES Bottle and low-resolution CTD dataset, Extractions 22 DEC 2013 (for years 1990-20012), 25 FEB 2015 (for year 2013), 13 OCT 2016 (for year 2015), 15 JAN 2019 (for years 2016-2017), 22 SEP 2020 (for year 2018), 10 MAR 2021 (for years 2019-202), 28 FEB 2022 (for year 2021), ICES, Copenhagen, 2022

IPCC: Climate Change 2021: The Physical Science Basis. Working Group I Contribution to the IPCC Sixth Assessment Report. doi:10.1017/9781009157896, 2021

Kniebusch, M., Meier, H. M., Neumann, T., Börgel, F. Temperature variability of the Baltic Sea since 1850 and attribution to atmospheric forcing variables. Journal of Geophysical Research: Oceans, 124(6), 4168-4187, https://doi.org/10.1029/2018JC013948, 2019a

Kniebusch, M., Meier, H. E. M., Radtke, H.: Changing salinity gradients in the Baltic Sea as a consequence of altered freshwater budgets. Geophys. Res. Lett., 46, 9739–9747, https://doi.org/10.1029/2019GL083902, 2019b

Lehmann, A., Myrberg, K., Post, P., Chubarenko, I., Dailidiene, I., Hinrichsen, H.-H., Hüssy, K., Liblik, T., Meier, H. E. M., Lips, U., Bukanova, T.: Salinity dynamics of the Baltic Sea. Earth Syst. Dynam., 13(1), 373–392, https://doi.org/10.5194/esd-13-373-2022, 2022

Leppäranta, M., Myrberg, K.: Physical Oceanography of the Baltic Sea. Springer-Verlag, 378 pp., ISBN 978-3-540-79702-9, 2009

Lindenthal, A., Hinrichs, C., Jandt-Scheelke, S., Kruschke, T., Lagemaa, P., van der Lee, E. M., Maljutenko, I., Morrison, H. E., Panteleit, T. R., and Raudsepp, U.: Baltic Sea surface temperature analysis 2022: a study of marine heatwaves and overall high seasonal temperatures, in: 8th edition of the Copernicus Ocean State Report (OSR8), edited by: von Schuckmann, K., Moreira, L., Grégoire, M., Marcos, M., Staneva, J., Brasseur, P., Garric, G., Lionello, P., Karstensen, J., and Neukermans, G., Copernicus Publications, State Planet, 4-osr8, 16, https://doi.org/10.5194/sp-4-osr8-16-2024, 2024.

Lindstrom, E., Gunn, J., Fischer, A., McCurdy, A., Glover, L. K.: A Framework for Ocean Observing. Task Team for an Integrated Framework for Sustained Ocean Observing, https://doi.org/10.5270/OceanObs09-FOO, 2012

Lu, Y., Li, Y., Lin, P., Duan, J., Wang, F.: North Atlantic–Pacific salinity contrast enhanced by wind and ocean warming. Nat. Clim. Chang., 14(7), 723–731, https://doi.org/10.1038/s41558-024-02033-y, 2024

McGrath, M., Poynting, M., Rowlatt, J.: Climate change: World's oceans suffer from record-breaking year of heat. BBC News Climate & Science, Retrieved from https://www.bbc.com/news/science-environment-68921215, 2024

Meier, H. E. M., Kauker, F.: Modeling decadal variability of the Baltic Sea: 2. Role of freshwater inflow and large-scale atmospheric circulation for salinity. J. Geophys. Res., 108, 3368, https://doi.org/10.1029/2003JC001799, 2003

Meier, H. E. M., Dieterich, C., Gröger, M., Dutheil, C., Börgel, F., Safonova, K., Christensen, O. B., Kjellström, E.: Oceanographic regional climate projections for the Baltic Sea until 2100. Earth Syst. Dynam., 13, 159–199, https://doi.org/10.5194/esd-13-159-2022, 2022

Meyssignac, B., Boyer, T., Zhao, Z., Hakuba, M.Z., Landerer, F.W., Stammer, D., Köhl, A., Kato, S., L'ecuyer, T., Ablain, M., Abraham, J.P.: Measuring global ocean heat content to estimate the Earth energy imbalance. Front. Mar. Sci., 6, 432, https://doi.org/10.3389/fmars.2019.00432, 2019

Mohrholz, V.: Major Baltic inflow statistics–revised. Front. Mar. Sci., 5, 384, https://doi.org/10.3389/fmars.2018.00384, 2018

Nontapa, C., Kesamoon, C., Kaewhawong, N., Intrapaiboon, P.: A New Time Series Forecasting Using Decomposition Method with SARIMAX Model. In: Yang, H., Pasupa, K., Leung, A.C.S., Kwok, J.T., Chan, J.H., King, I. (eds). Neural Information Processing. Commun. Comput. Inf. Sci., vol 1333, Springer, Cham, https://doi.org/10.1007/978-3-030-63823-8_84, 2020

Panteleit, T., Verjovkina, S., Jandt-Scheelke, S., Spruch, L., Huess, V.: EU Copernicus Marine Service Quality Information Document for the Baltic Sea Physics Reanalysis Product. Mercator Ocean International, https://catalogue.marine.copernicus.eu/documents/QUID/CMEMS-BAL-QUID-003-011.pdf, last access: 12 April 2023

Radtke, H., Brunnabend, S.-E., Gräwe, U., Meier, H. E. M.: Investigating interdecadal salinity changes in the Baltic Sea in a 1850–2008 hindcast simulation. Clim. Past, 16, 1617–1642, https://doi.org/10.5194/cp-16-1617-2020, 2020

Ranasinghe, R., Ruane, A.C., Vautard, R., Arnell, N., Coppola, E., Cruz, F.A., Dessai, S., Islam, A.S., Rahimi, M., Ruiz Carrascal, D., Sillmann, J., Sylla, M.B., Tebaldi, C., Wang, W., Zaaboul, R.: Climate Change Information for Regional Impact and for Risk Assessment. In: Masson-Delmotte, V., Zhai, P., Pirani, A., Connors, S.L., Péan, C., Berger, S., et al. (eds.). Climate Change 2021: The Physical Science Basis. Working Group I Contribution to the IPCC Sixth Assessment Report. Cambridge University Press, https://doi.org/10.1017/9781009157896.014, 2021

Raudsepp, U., Maljutenko, I.: A method for assessment of the general circulation model quality using K-means clustering algorithm: A case study with GETM v2.5. Geosci. Model Dev., 15, 535–551, https://doi.org/10.5194/gmd-15-535-2022, 2022

Raudsepp, U., Maljutenko, I., Barzandeh, A., Uiboupin, R., and Lagemaa, P.: Baltic Sea freshwater content, in: 7th edition of the Copernicus Ocean State Report (OSR7), edited by: von Schuckmann, K., Moreira, L., Le Traon, P.-Y., Grégoire, M., Marcos, M., Staneva, J., Brasseur, P., Garric, G., Lionello, P., Karstensen, J., and Neukermans, G., Copernicus Publications, State Planet, 1-osr7, 7, https://doi.org/10.5194/sp-1-osr7-7-2023, 2023.

Raudsepp, U., Maljutenko, I., Haapala, J., Männik, A., Verjovkina, S., Uiboupin, R., von Schuckmann, K., Mayer, M.: Record high heat content and low ice extent in the Baltic Sea during winter 2019/20. In: Copernicus Ocean State Report, Issue 6, Journal of Operational Oceanography, 15:sup1, s175–s185; DOI:10.1080/1755876X.2022.2095169, 2022.

Ringgaard, I., Korabel, V., Spruch, L., Lindenthal, A., Huess, V.: EU Copernicus Marine Service Product User Manual for the Baltic Sea Physics Reanalysis Product. Mercator Ocean International, https://catalogue.marine.copernicus.eu/documents/PUM/CMEMS-BAL-PUM-003-011_012.pdf, last access: 1 July 2024

Rodhe, J., Winsor, P.: On the influence of the freshwater supply on the Baltic Sea mean salinity, Tellus A: Dynamic Meteorology and Oceanography, 54:2, 175-186, DOI:10.3402/tellusa.v54i2.12134, 2002.

Schubert, S.D., Chang, Y., DeAngelis, A.M., Koster, R.D., Lim, Y-K., Wang, H.: Exceptional Warmth in the Northern Hemisphere during January–March of 2020: The Roles of Unforced and Forced Modes of Atmospheric Variability. J. Clim., 35(8), 2565–2584, https://doi.org/10.1175/JCLI-D-21-0291.1, 2022

Safonova, K., Meier, H.E.M., Gröger, M.: Summer heatwaves on the Baltic Sea seabed contribute to oxygen deficiency in shallow areas. Commun. Earth Environ., 5, 106, https://doi.org/10.1038/s43247-024-01268-z, 2024

Savchuk, P.: Large-Scale Nutrient Dynamics in the Baltic Sea, 1970–2016. Front. Mar. Sci., 5, 95, https://doi.org/10.3389/fmars.2018.00095, 2018

Schauer, U., Losch, M. Freshwater in the ocean is not a useful parameter in climate research. Journal of Physical Oceanography, 49(9), 2309–2321, https://doi.org/10.1175/JPO-D-19-0102.1, 2019

Skliris, N., Marsh, R., Josey, S.A., Good, S.A., Liu, C., Allan, R.P.: Salinity changes in the World Ocean since 1950 in relation to changing surface freshwater fluxes. Clim. Dyn., 43(3-4), 709–736, https://doi.org/10.1007/s00382-014-2131-7, 2014

Solomon, A., Heuzé, C., Rabe, B., Bacon, S., Bertino, L., Heimbach, P., Inoue, J., Iovino, D., Mottram, R., Zhang, X., Aksenov, Y., McAdam, R., Nguyen, A., Raj, R. P., and Tang, H.: Freshwater in the Arctic Ocean 2010–2019, Ocean Sci., 17, 1081–1102, https://doi.org/10.5194/os-17-1081-2021, 2021

Uotila, P., Vihma, T., Haapala, J.: Atmospheric and oceanic conditions and the extremely low Bothnian Bay sea ice extent in 2014/2015. Geophys. Res. Lett., 42, 7740–7749, https://doi.org/10.1002/2015GL064901, 2015

von Schuckmann, K., Palmer, M., Trenberth, K. et al. An imperative to monitor Earth's energy imbalance. Nature Clim Change 6, 138–144, https://doi.org/10.1038/nclimate2876, 2016

von Schuckmann, K., Minière, A., Gues, F., Cuesta-Valero, F. J., Kirchengast, G., Adusumilli, S., Straneo, F., Ablain, M., Allan, R. P., Barker, P. M., Beltrami, H., Blazquez, A., Boyer, T., Cheng, L., Church, J., Desbruyeres, D., Dolman, H., Domingues, C. M., García-García, A., Giglio, D., Gilson, J. E., Gorfer, M., Haimberger, L., Hakuba, M. Z., Hendricks, S., Hosoda, S., Johnson, G. C., Killick, R., King, B., Kolodziejczyk, N., Korosov, A., Krinner, G., Kuusela, M., Landerer, F. W., Langer, M., Lavergne, T., Lawrence, I., Li, Y., Lyman, J., Marti, F., Marzeion, B., Mayer, M., MacDougall, A. H., McDougall, T., Monselesan, D. P., Nitzbon, J., Otosaka, I., Peng, J., Purkey, S., Roemmich, D., Sato, K., Sato, K., Savita, A., Schweiger, A., Shepherd, A., Seneviratne, S. I., Simons, L., Slater, D. A., Slater, T., Steiner, A. K., Suga, T., Szekely, T., Thiery, W., Timmermans, M.-L., Vanderkelen, I., Wjiffels, S. E., Wu, T., and Zemp, M.: Heat stored in the Earth system 1960–2020: where does the energy go?, Earth Syst. Sci. Data, 15, 1675–1709, https://doi.org/10.5194/essd-15-1675-2023, 2023

Winsor, P., Rodhe, J., Omstedt, A.: Baltic Sea ocean climate: an analysis of 100 yr of hydrographic data with focus on the freshwater budget. Climate Research, 18(1/2), 5–15. http://www.jstor.org/stable/24861552, 2001

Appendix 1

We also examined the fit of the trend-included time series and their correspondence with meteorological variables for OHC and FWC (Figure A1). The correlation coefficient and RMSD for the OHC model are 0.9537 and 0.4310, respectively; for FWC model, they are 0.8897 and 0.5994.

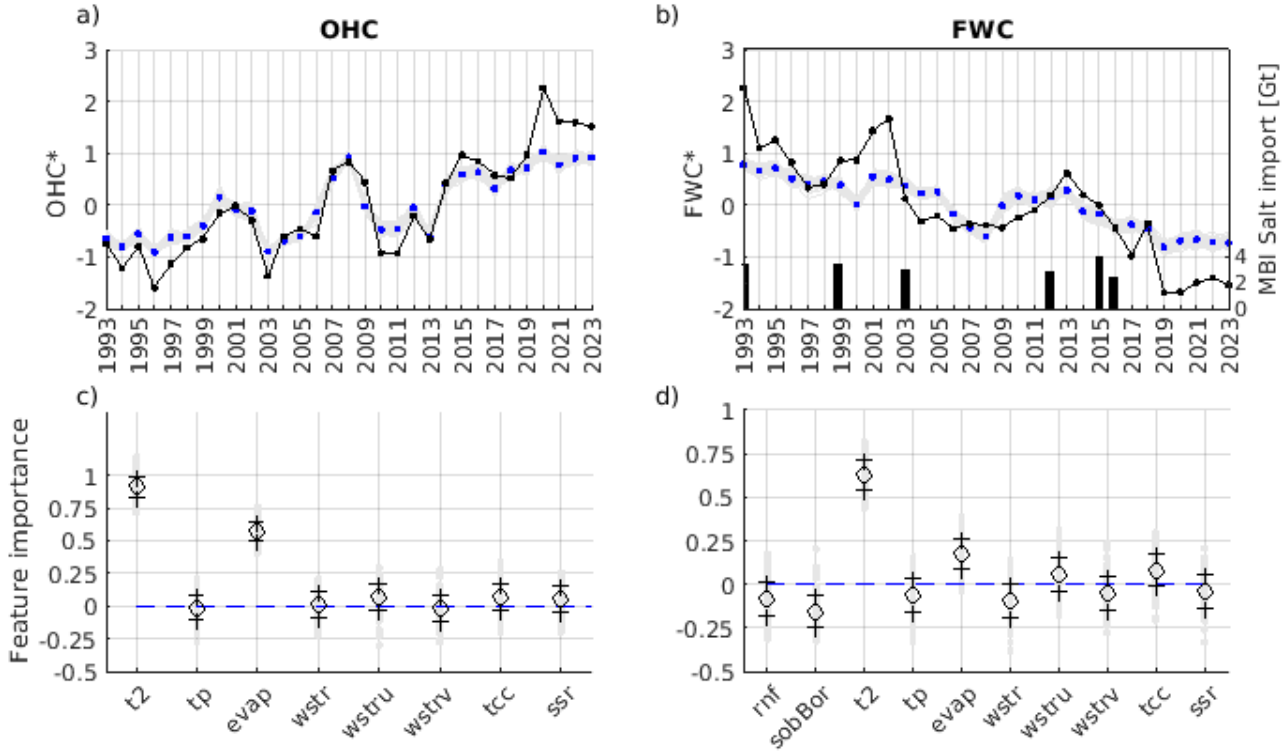

Figure A1. Same as in Figure 4, but the RF_*var models are fit for the original FWC and OHC including trends.

Appendix 2

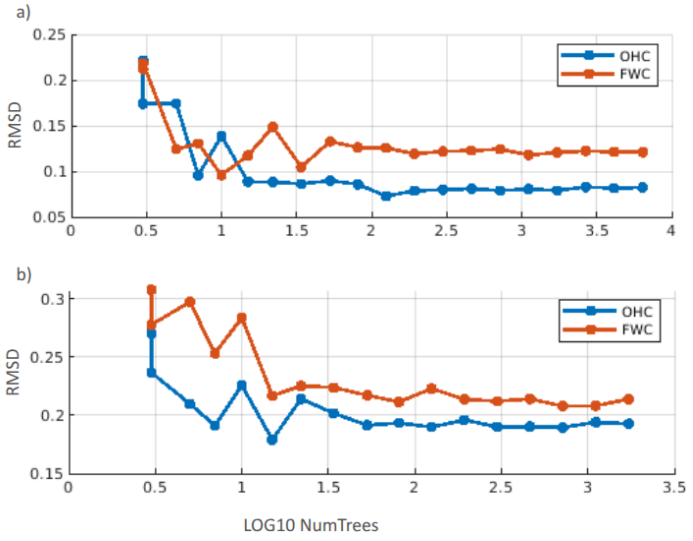

Figure A2. Random forest models for *zax a) and *var b) sensitivity to $\log_{10}$ of the number of trees (NumTrees)